

Application Report

Voltage-gated sodium channels on QPatch

HEK- $\text{Na}_v1.2a$ & $1.5a$ - whole-cell current data used for ion channel characterization

Summary

Biophysical characterization of fast voltage-gated sodium channels by QPatch.

- Current-voltage analysis
- Inactivation and Boltzmann fits
- Concentration-response assays
- Screening: pore block vs state-dependent block
- Frequency dependence
- Recovery from inactivation

In collaboration with NeuroSearch and GlaxoSmithKline.

Introduction

This report presents QPatch whole-cell current recordings from fast voltage-gated Na^+ channel data from two studies:

- HEK293 cells stably expressing the rat $\text{Na}_v1.2a$. Experiments were conducted at Sophion Bioscience for GlaxoSmithKline, Verona, Italy
- HEK293 cells stably expressing rat $\text{Na}_v1.2a$ or $\text{Na}_v1.5a$. Experiments were conducted at NeuroSearch, Ballerup, Denmark

The extracellular Ringer's solution contained 140 mM Na^+ , whereas the intracellular Ringer's solution was Na^+ -free, the major cation being Cs^+ at a concentration of 120 mM. Experiments were conducted at room temperature (21°C).

Results

Current-voltage relation and inactivation characteristics

1A shows a family of Na^+ currents in response to depolarizing pulses from -90 to 70 mV (see inset).

The holding potential was -90 mV. Currents were filtered at 4 kHz and sampled at 50 kHz.

Fig. 1B shows the resulting I-V relationship for peak Na^+ channel currents. The activation threshold was -40 mV, and the maximal current amplitude was obtained at -10 mV. At large positive membrane potentials the current amplitude is reduced as the electrochemical driving force vanishes.

Fig. 1C shows the inactivation graph for the Na^+ channel. The membrane potential was held at a holding potential of -90 mV, subsequently shifted to conditioning potentials ranging from -160 to 0 mV for 1000 ms, and finally the current was measured upon a step to 0 mV (see inset). The resulting current amplitude indicates the fraction of Na^+ channels in the inactivated state. At potentials more negative than -80 mV the channels were predominantly in the closed state (before the conditioning pulse), whereas at potentials above -40 mV they were predominantly in the inactivated state (before the conditioning pulse). The red curve represents the Boltzmann fit from which the $V_{0.5}$ for steady-state inactivation was estimated to -59 mV.

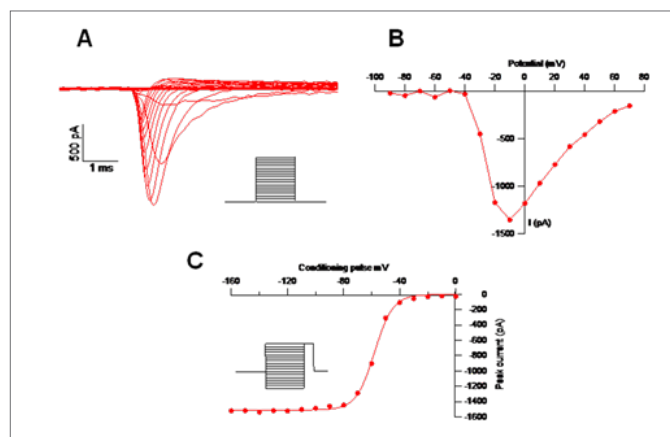


Fig. 1. A) Na^+ -current in response to depolarizing steps; voltage protocol shown in the inset. B) I-V relationship of the Na^+ -current shown in A). C) I-V relationship of the steady-state inactivation of the Na^+ -channel. Voltage protocol shown in the inset.

Concentration-response relation for tetrodotoxin

The effect of tetrodotoxin (TTX) on Na_v1.2a (Fig. 2A) and Na_v1.5a (Fig. 2B) whole-cell currents was explored by application of four increasing blocker concentrations.

Fig. 2 shows the raw current responses (top), the effect on Na⁺ current peak amplitudes during the four TTX applications (I-t relation) as seen with the QPatch Assay Software (middle), and the resulting concentration-response relationship (bottom) for Na_v1.2a and Na_v1.5a, respectively.

It is seen that IC₅₀ for TTX was a hundredfold higher in the case of Na_v1.5a than in the case of Na_v1.2a: 1.1 μM vs. 11 nM (N=3-6). The Hill coefficients (n_{Hill}) were similar for the two concentration-response relationships.

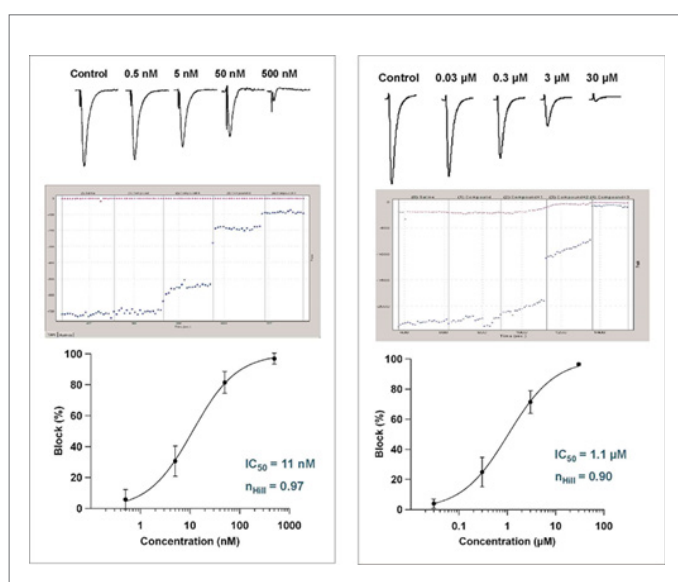


Fig. 2. Left: Na_v1.2a responses to increasing concentrations of TTX. Upper panel: Raw current traces, middle panel: I-t plot, lower panel: Hill fit. Right: Na_v1.5 responses to increasing concentrations of TTX. Upper panel: Raw current traces, middle panel: I-t plot, lower panel: Hill fit.

Identification of state-dependent inhibitors

To explore state-dependency of channel block, the cell was depolarised twice with a temporal separation of 15 ms (Fig. 3A). The current-time relationship for the peak Na⁺ currents recorded in response to the first (blue) and the second (magenta) depolarisation is shown in Fig. 3B. It is seen that the employed compound (lidocaine) inhibited the channel in the inactivated state only (second lane). The effect of the compound was reversible (third lane). Subsequent addition of TTX (fourth lane) blocked both currents equally. The currents partly recovered from the TTX block (fifth lane).

Ten compounds were tested for potential state-dependent effects on Na_v1.2a and Na_v1.5a (see Fig. 4). It is seen that NS-X exhibited the highest degree of state-dependence on both Na_v1.2a and Na_v1.5a. Generally, the state-dependency of blocker action was more pronounced for Na_v1.5a than for Na_v1.2a. Only the effect of TTX was completely state-independent. The amplitudes of Na⁺ currents were normalized to the level just prior to compound application (saline). The control experiments were conducted without drug.

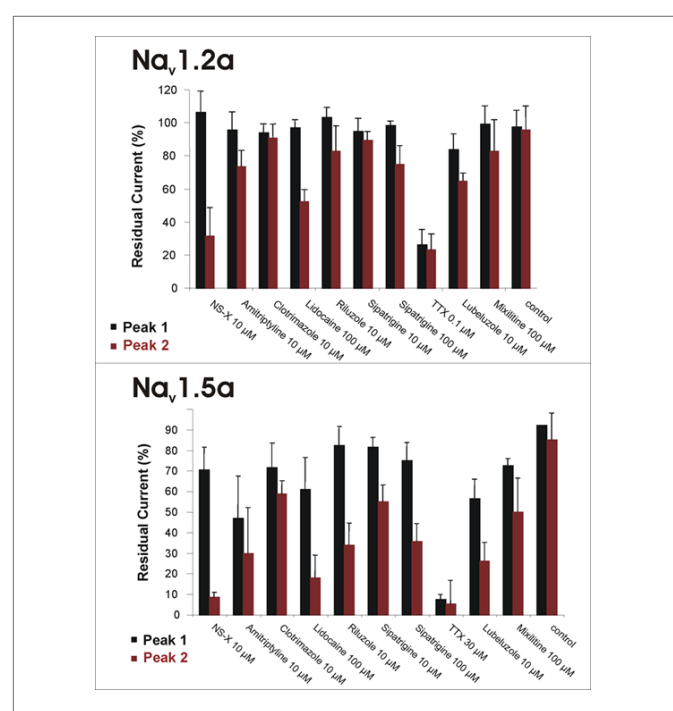


Fig. 3. Na-current amplitudes normalized to saline response for peak 1 and 2 in the voltage protocol shown in Fig. 3.

Frequency-dependent block by riluzole

To test for frequency-dependence of blockade, trains of 40 depolarisation pulses (2 ms from a holding potential of -110 to 0 mV) were executed at 100 Hz in the absence and presence of riluzole at 4 concentrations ranging from 0.3 to 300 μM (Fig. 5, left panel). The effect of increasing concentrations of riluzole on Na⁺ current amplitudes is seen in the right panel of Fig. 5 (normalized currents).

It is seen that increasing concentrations of riluzole suppresses steady-state (>~20 pulses) current amplitudes.

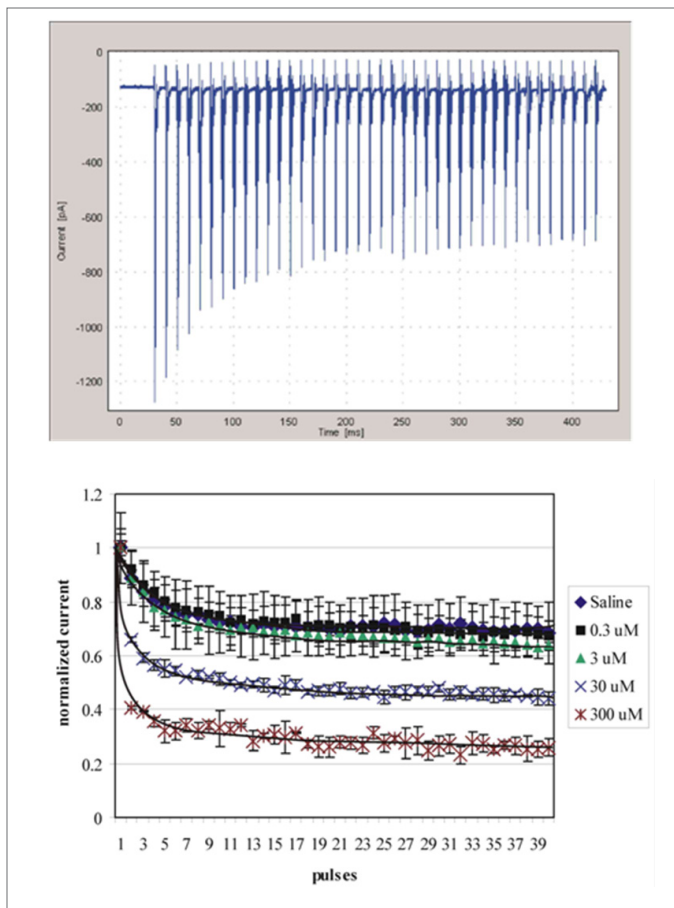


Fig. 4. Frequency dependent block of Na-current by riluzole

Drug effects on recovery from inactivation

Fig. 6 shows Nav1.2a channel currents in response to 20 ms depolarisations from -90 to 0 mV elicited at varying intervals (Δt), ranging from 1 to 1000 ms, after an initial 100 ms depolarisation (upper panel). Lower panel shows the effect of lidocaine on these currents.

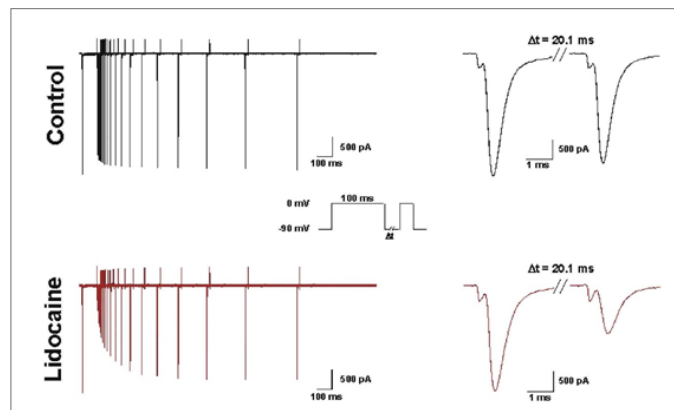


Fig. 5. Upper panel shows a control experiment of Nav1.2a channel current elicited using the voltage protocol shown on the right. The time to the second pulse was incrementally increased. The lower panel shows the experiment conducted with lidocaine.

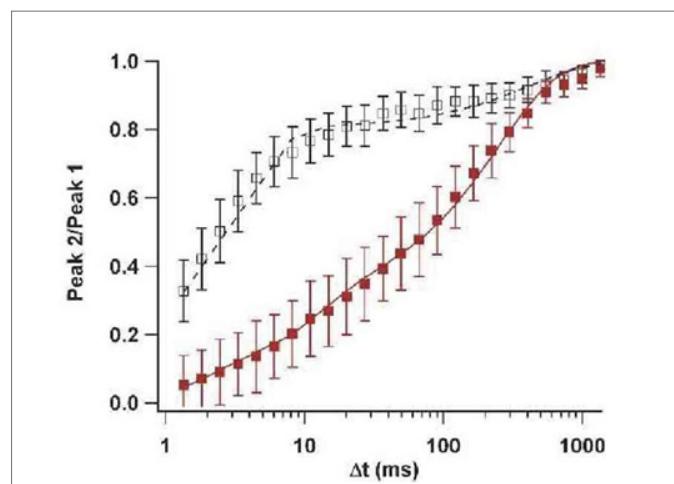


Fig. 6. Plot of the ratio between the first and second current spike elicited with the voltage protocol shown in Fig. 6. White squares represent control experiments and red squares represent experiments with lidocaine.

It is seen that lidocaine prolongs recovery from inactivation. It significantly reduces the amplitudes of Na⁺ currents elicited in response to depolarisations executed at short time-intervals ($\Delta t < 300$ ms) subsequent to the initial depolarisation. The ratio between the amplitudes of the initial and the subsequent Na⁺ current spikes is shown in Fig. 7.

Conclusion

The results demonstrate that QPatch 16 can provide high-quality whole-cell current data from fast voltage-activated Na⁺ channels, and that protocols can be defined that allow analysis of drug potency (IC_{50}), inactivation kinetic properties, as well as state- and frequency-dependency of drug action.